Effect of Silicon Content over Fe-Cu-Si/C Based Composite Anode for Lithium Ion Battery

Chil-Hoon Doh,[†,*] Hye-Min Shin,[†,‡] Dong-Hun Kim,[†,§] Young-Dong Chung,[†] Seong-In Moon,[†] Bong-Soo Jin,[†] Hyun-Soo Kim,[†] Ki-Won Kim,[§] Dae-Hee Oh,[‡] and Angathevar Veluchamy[†,#]

[†]*Korea Electrotechnology Research Institute, Changwon 641-600, Korea.* [*]*E-mail: chdoh@keri.re.kr*
[‡]*Pukyong National University, Pusan 608-739, Korea*
[§]*Gyeonsang National University, Jinju 660-701, Korea*
[#]*Central Electrochemical Research Institute, Karaikudi 630 006, India*
Received June 30, 2007

Two different anode composite materials comprising of Fe, Cu and Si prepared using high energy ball milling (HEBM) were explored for their capacity and cycling behaviors. Prepared powder composites in the ratio Cu:Fe:Si = 1:1:2.5 and 1:1:3.5 were characterized through X-Ray diffraction (XRD) and scanning electron microscope (SEM). Nevertheless, the XRD shows absence of any new alloy/compound formation upon ball milling, the elements present in Cu(1)Fe(1)Si(2.5)/Graphite composite along with insito generated Li_2O demonstrate a superior anodic behavior and delivers a reversible capacity of 340 mAh/g with a high coulombic efficiency (98%). The higher silicon content Cu(1)Fe(1)Si(3.5) along with graphite could not sustain capacity with cycling possibly due to ineffective buffer action of the anode constituents.

Key Words : High energy mechanical milling, Fe(1)Cu(1)Si(3.5), Fe(1)Cu(1)Si(2.5), Anode, Li-ion battery

Introduction

The rapid growth of electronic industries and electric vehicle applications has accelerated the need for high energy and long life lithium ion batteries. Recently, attempts have been made to enhance the energy density and cycle life of both anode and cathode. Since graphite anode has only 372 mAh g^{-1} [1] as energy density, anodes such as tin (Sn) and silicon (Si) with high theoretical capacities 4190 and 990 mAh g^{-1} for the respective intermetallic alloys $Li_{22}Si_5$ and $Li_{22}Sn_5$ have been considered. The practical application of these materials has been hampered as they exhibit wide volume variations, 328% for Li-Si and 258% for Li-Sn during discharge/charge processes which leads the electrodes to undergo internal cracks and morphological changes resulting in loss of electrical contact and cell failure.[2] In order to identify a suitable anode material with high electrochemical characteristics intermetallic silicide alloys with less active or inactive metal elements with two metals,[3-20] carbon coated silicon[21,22] and alloys consisting of multi-components[23,27] were explored mostly with ductile graphite.

In this paper two different composites constituting of Fe, Cu and Si, with different silicon contents have been considered. This combination has been chosen in order to make use of conducting property of copper along with environmentally benign elements, Iron and silicon. The synthesis procedure uses High Energy Ball Mill technique (HEBM) to prepare Fe-Cu-Si composite in the presence and absence of super 'p' black and graphite. X-Ray diffraction (XRD) and Scanning Electron Microscope (SEM) were employed to analyze the structure and morphology of the materials.

Experimental Details

Material preparation. Two different Fe-Cu-Si ternary composites were prepared by adopting HEBM technique. Appropriate quantities of Cu (< 10 μm, 99% pure, Sigma Aldrich), Fe (< 53 μm, 99.9% pure, High purity chemical research company, Japan) and Si (1-5 μm, SI-100, > 99% purity, AEE, N.J) were loaded in a stainless steel (SS) grinding vial along with SS balls. The weight ratio of SS ball to material was maintained at 10:1 and the millings were performed at 350 rpm for 10 hours. The vial was filled with argon gas and tightly closed with a gasket to prevent oxidation of the loaded material through any possible ingress of atmospheric air into the vial.

The active material (AM_1) with atomic ratio Fe:Cu:Si = 1:1:3.5 was ball milled. A mix consisting of AM_1:Super 'p' black (SPB) in the ratio = 75:15 was blended in an agate mortar and a viscous slurry was prepared by blending with 10 wt % polyvinylidene difluoride (PVDF) dissolved in 1-methyl-2-pyrrolidinone using an agitator for 10 minutes. Following the same procedure also made another slurry composition using the same active material (AM_1) as AM_1: Graphite:SPB:PVDF = 45:35:10:10. Similarly one more active material (AM_2) containing less amount of silicon with atomic ratio Fe:Cu:Si = 1:1:2.5 was ball milled as before and viscous slurry with AM_2:Graphite:SPB:PVDF = 40:40:10:10 was prepared. Three different viscous slurries were coated on different copper foils and dried in a vacuum oven at 150 °C for 24 h. The films were removed and pressed using SS roller so as to reduce the thickness to 75%. For convenience here afterwards, it may be denoted Fe:Cu:Si = 1:1:3.5 and Fe:Cu:Si = 1:1:2.5 as Fe(1)Cu(1)Si(3.5) and Fe(1)Cu(1)

Si(2.5) respectively.

Cell construction. The coated films were cut in the form of circular disc of diameter 1.4 cm using a die. Coin cell was fabricated using the coated film and lithium foil separated by polypropylene membrane, celgard 2700 as a separator. The electrolyte used was as received from Techno Semichem. Ltd., Korea. The electrolyte is 1 M $LiPF_6$ and 2 wt% vinylene carbonate (VC) dissolved in a mixed solution of ethylene carbonate (EC) and ethyl methyl carbonate (EMC) = 1: 1(V/V)). The coin cells were assembled in a dry room maintained at ~21 °C with a dew point temperature between −65 and −70 °C.

XRD and SEM investigations. In order to obtain the phase characterization, ball milled composites were examined using Philips 1830 X-ray diffractometer with nickel filtered Cu Kα radiation at a scan rate of 0.04°/s over 2 theta range 10°-80°. The surface morphology of the active material coated copper foil was scanned using Hitachi S-4800 scanning electron microscope.

Cycle life testing. Discharge-charge studies and cycle life measurements of the coin cells were carried out using Charge-discharge analyzer, Toyo System, LTD, Japan. The anode was cycled between 0 to 2 V versus Li^+/Li at a constant current of 0.253 mA cm^2.

Results and Discussion

Phase and morphology analyses

X-Ray diffraction of the ball milled sample: In Figure 1, the XRD pattern for the elemental Si, Cu, Fe powders along with 10 h ball milled composite Fe(1)Cu(1)Si(3.5) and Fe(1)Cu(1)Si(2.5), are presented. It is found that the XRD pattern of individual elements such as Si, Cu and Fe exactly superimpose with the spectrums obtained for 10 h ball milled composites Fe(1)Cu(1)Si(3.5) and Fe(1)Cu(1)Si(2.5). This observation suggests that the resultant material remains as a composite with changes only in crystallite sizes and does not form any new compound or alloys due to ball milling. The following section describes the reaction of Si during lithiation and delithiation, and other elements in providing buffer action for a stable charge-discharge cycle behavior.

SEM analysis: The high silicon containing electrodes of

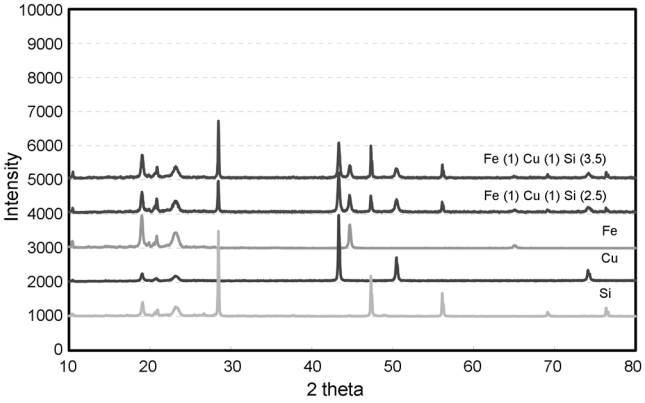

Figure 1. XRD profile of Fe, Cu, Si and 10 h ball milled composites, Fe(1)Cu(1)Si(3.5) and Fe(1)Cu(1)Si(2.5).

composition Fe(1)Cu(1)Si(3.5) composite with SPB, Fe(1) Cu(1)Si(3.5)/Graphite composite and low silicon containing composite Cu(1)Fe(1)Si(2.5)/Graphite composite are shown in the SEM picture. The appearance of nano particles in 'a' is due to the presence of SPB which was added as a conducting material. The electrode 'b' shows larger size active material particles. The SEM pictures show that the particle distribution in 'c' is significantly better than that in 'a' and 'b' for favorable buffer action to provide high cycle capacity.

Electrochemical characterization

Discharge/charge behavior of Fe(1)Cu(1)Si(3.5) composite: The Figure representing charge/discharge behavior of Fe(1)Cu(1)Si(3.5) blended with conducting material SPB is shown as Figure 3. The figure shows the initial discharge and charge capacity values as 1758 and 1133 mAh g^{-1} respectively. Two types of reactions occur in the cell.

1) The reversible charge/discharge reaction

$$(x+y)Li^+ + (Si, Fe, Cu, C) + (x+y)e^- \leftrightarrow Li_xSi + Li_yC_6 + (Fe, Cu) \quad (1)$$

Li and graphite can undergo reversible reaction with Silicon. This composition contain no graphite and the SPB acts only as a conduction material. Other elements serves as a buffer to obsorb the volume expansion during charge-discharge process.

2) The irreversible reaction occurs during initial discharge

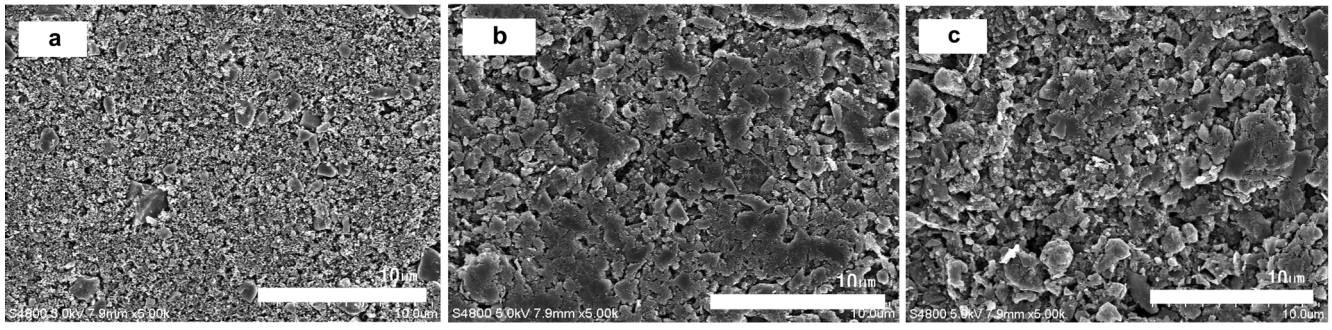

Figure 2. SEM pictures for the electrodes with compositions, a) Fe (1)Cu(1)Si(3.5) composite with SPB, b) Fe(1)Cu(1)Si(3.5)/Graphite composite, c) Fe(1)Cu(1)Si(2.5)/Graphite composite.

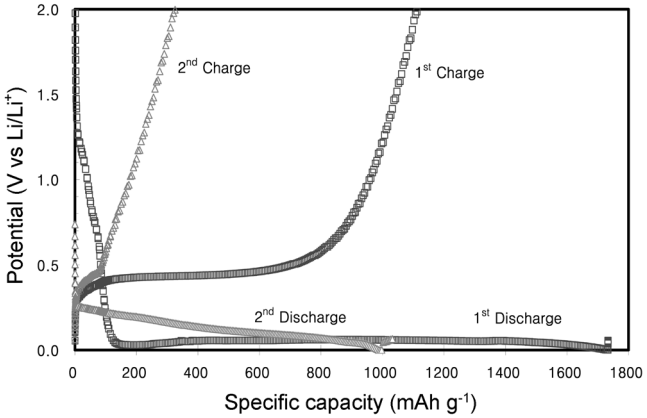

Figure 3. Potential as a function of specific capacity for Fe(1)Cu (1)Si(3.5) composite.

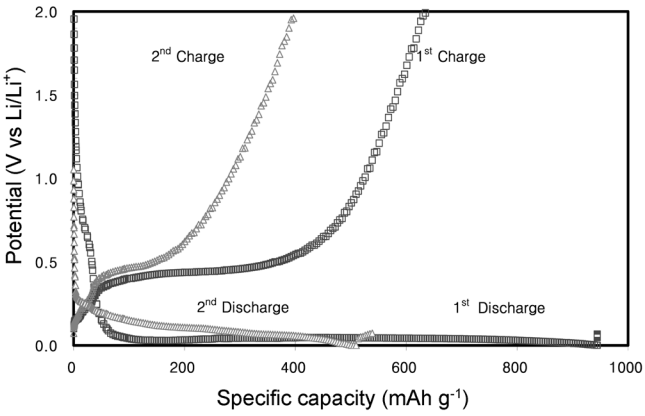

Figure 4. Potential as a function of specific capacity for Fe(1)Cu (1)Si(3.5)/Graphite composite.

$$2Li^+ + \text{-O-} + 2e^- \rightarrow Li_2O \quad (2)$$

-O- derives from chemically bonded/adsorbed oxides

In the first discharge process lithium equivalent to 625 mAh g^{-1} has been converted to Li_2O[28] which remains in the anode as irreversible capacity which is then followed by reversible lithium silicide alloy formation. It is reported that the irreversible capacity in graphite electrode has been attributed to the formation of a passive film on graphite particles which comprises mainly LiF, Li_2CO_3 and Li_2O.[16,29] In the present composite the elements Cu and Fe along with Li_2O act as a buffer to absorb the volume changes during charge and discharge process. The percentage of irreversible capacity for the first cycle is 35% and for the second cycle is 65%. The drop in capacity in the second charge implies that this composition is not able to provide sufficient buffer action to give long cycle life for this composition.

Discharge/charge behavior of Fe(1)Cu(1)Si(3.5)/Graphite composite: The charge/discharge curve represented as in Figure 4 shows that the initial capacity is below 1000 mAh g^{-1} which is lower than the capacity delivered by Fe(1)Cu(1)Si(3.5) composite with SPB. However, the second charge capacity remains higher at ~400 mAh g^{-1} which is far above the value exhibited by the composition with SPB (Fig. 3). In this composite the graphite is responsible for lowering of initial capacity and maintaining of higher capacity in the following cycles.

Discharge/charge behavior of Fe(1)Cu(1)Si(2.5)/Graphite composite: The discharge/charge behavior of Fe(1) Cu(1)Si(2.5)/Graphite shown in Figure 5 illustrates that even though the initial capacity is reduced to ~800 mAh g^{-1}, the second charge capacity remains > 500 mAh g^{-1}.

Comparative delithiation behavior of different compositions: Since delithiation characteristics are more important as it is related to the amount of lithium available for lithiation process in practical lithium ion battery, the comparative delithiation behavior of three compositions are presented as in Figure 6. The curve 'a' obtained for the composite Fe(1)Cu(1)Si(3.5)/SPB containing high silicon content does not provide good cycle life possibly due to large volume expansion and crumbling of the active material net work and loss of electrical contact with cycling. However, the same composite when added graphite as Fe(1) Cu(1)Si (3.5)/Graphite shown as 'b' was able to prolong the cycle life but at the cost of capacity. The figure clearly shows

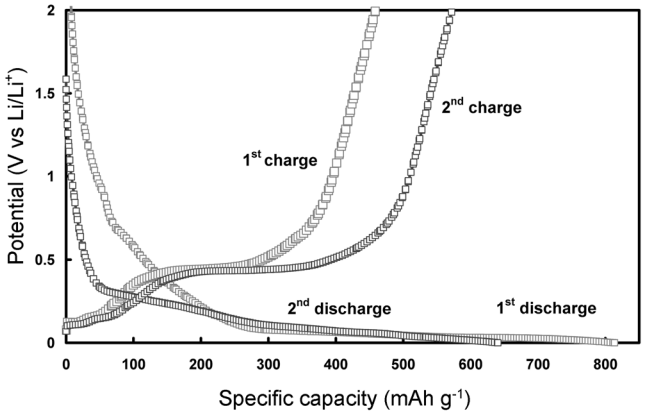

Figure 5. Potential as a function of specific capacity for Fe(1)Cu (1)Si(2.5)/Graphite composite.

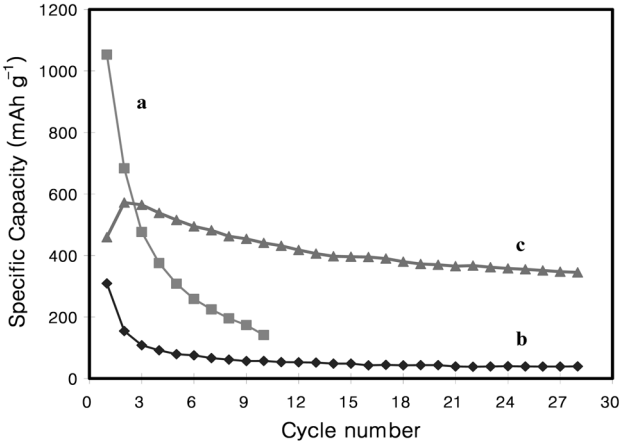

Figure 6. Specific capacity as a function of cycle number for a) Fe (1)Cu(1)Si(3.5) composite with SPB, b) Fe(1)Cu(1)Si(3.5)/ Graphite composite, c) Fe(1)Cu(1)Si(2.5)/Graphite composite.

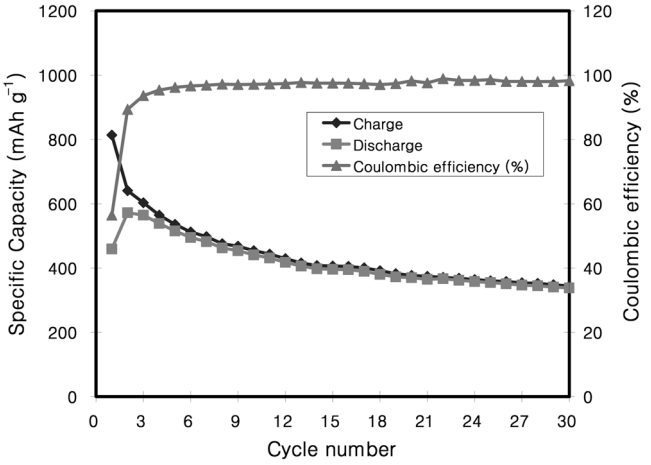

Figure 7. Charge/discharge and coulombic efficiency as a function of cycle number for Fe(1)Cu(1)Si(2.5)/Graphite composite.

that the composition Fe(1)Cu(1)Si(2.5)/Graphite shown as 'c' depicts better capacity and high cycle life. The high performance of the Fe(1)Cu(1)Si(2.5)/Graphite is due to the effective buffer action provided along with internally generated Li_2O during first lithiation process. Consequently these materials can be considered as a double phase material as both silicon and graphite are active towards Li^+ within the same potential window.[2] It needs further investigation to see exactly the beneficial effect of copper over the discharge/charge characteristics of the final composite arrived.

Cycle behavior and coulombic efficiency: The cycle behavior and coulombic efficiency of the composite Cu(1) Fe(1)Si(2.5)/Graphite presented as in Figure 7 shows that at 30th cycle the coulombic efficiency is > 98% and the specific capacity is ~340 mAh g^{-1}. The electrochemical behavior of this composite is comparable to the results reported for $LiFePO_4$ and $Fe_{0.92}Mn_{0.08}Si_2$ as anode materials with reversible capacity of ~300 and ~400 mAh g^{-1} at 20th and 25th cycles respectively.[26,30]

Conclusion

Two different compositions prepared through ball milling in order to evaluate the electrochemical behavior of the composites for lithium ion battery. Despite the XRD analysis shows absence of any alloys/compounds formation due to ball milling, the elements present in Cu(1)Fe(1)Si(2.5)/Graphite composite along with insito generated Li_2O has shown a reversible capacity ~340 mAh/g, with high coulombic efficiency > 98%. Although the composite Cu(1)Fe(1)Si (3.5) with SPB and Cu(1)Fe(1)Si(3.5) with SPB & graphite are able to provide high initial capacity, could not sustain reasonable capacity with cycle life, possibly due to higher silicon content which causes higher volume expansion and affect the capacity with cycle life.

Acknowledgement. This work has been carried out at Division of Advanced Batteries supported by NGE program (Project No. 1001653) of KERI, Korea. One of the authors A. Veluchamy wishes to thank the Korean Federation of Science and Technology Societies, Korea for awarding Brain Pool Fellowship and also thanks CECRI/CSIR, India for granting extraordinary leave.

References

1. Yazami, R.; Zaghib, K.; Deschamps, M. *J. Power Sources* **1994**, *52*, 55.
2. Nikolay Dimov, Satoshi Kugino, Masaki Yoshio, *Electrochim. Acta* **2003**, *48*, 1579.
3. Wolfenstine, J. *Power Sources* **2003**, *124*, 241.
4. Wang, G. X.; Sun, L.; Bradhurst, D. H.; Zhong, S.; Dou, S. X.; Liu, H. K. *J. Power Sources* **2000**, *88*, 278.
5. Park, M. S.; Rajendran, S.; Kang, Y. M.; Han, K. S.; Han, Y. S.; Lee, J. Y. *J. Power Sources* **2006**, *158*, 650.
6. Park, M. S.; Lee, Y. J.; Han, Y. S.; Lee, J. Y. *Materials Letters* **2006**, *60*, 3079.
7. Wang, Z.; Tian, W. H.; Liu, X. H.; Li, Y.; Li, X. G. *Materials Chemistry and Physics* **2006**, *100*, 92.
8. Park, M. S.; Lee, Y. J.; Rajendran, S.; Song, M. S.; Kim, H. S.; Lee, J. Y. *Electrochim. Acta* **2005**, *50*, 5561.
9. Lee, H. Y.; Kim, Y. L.; Kong, M. K.; Lee, S. M. *J. Power Sources* **2005**, *141*, 159.
10. Kim, J. B.; Jun, B. S.; Lee, S. M. *Electrochim. Acta* **2005**, *50*, 3390.
11. Dong, H.; Feng, R. X.; Ai, X. P.; Cao, Y. L.; Yang, H. X. *Electrochim. Acta* **2004**, *49*, 5217.
12. Zuo, P.; Yin, G.; Tong, Y. *Solid State Ionics* **2006**, *177*, 3297.
13. Kim, Y. L.; Lee, H. Y.; Jang, S. W.; Lim, S. H.; Lee, S. J.; Baik, H. K.; Yoon, Y. S.; Lee, S. M. *Electrochim. Acta* **2003**, *48*, 2593.
14. Kim, H.; Choi, J.; Sohn, H. J.; Kang, T. *J. Electrochem. Soc.* **1999**, *146*, 440.
15. Roberts, G. A.; Cairns, E. J.; Reimers, J. A. *J. Power Sources* **2002**, *110*, 424.
16. NuLi, Y.; Wang, B.; Yang, J.; Yuan, X.; Ma, Z. *J. Power Sources* **2005**, *153*, 371.
17. Yoon, S.; Lee, S.; Kim, H.; Sohn, H. J. *J. Power Sources* **2006**, *161*, 1319.
18. Wu, X. D.; Wang, Z. X.; Chen, L. Q.; Huang, X. J. *Electrochem. Commun.* **2003**, *5*, 935.
19. Lee, Y. S.; Lee, J. H.; Kim, Y. W.; Sun, Y. K.; Lee, S. M. *Electrochimica Acta* **2006**, *52*, 1523.
20. Patel, P.; Kim, I. S.; Kumta, P. N. *Material Science and Engineering B* **2005**, *116*, 347.
21. Yun, M. S.; Jeong, K. Y.; Lee, E. W.; Doh, C. H. *Bull. Korean Chem. Soc.* **2006**, *27*, 1175.
22. Yun, M. S.; Jeong, K. Y.; Lee, E. W.; Jin, B. S.; Kim, H. S.; Moon, S. I.; Doh, C. H. *J. Chem. Eng.* **2006**, *23*, 230.
23. Weydanz, W. J.; Mehrens, M. W.; Huggins, R. A. *J. Power Sources* **1999**, *81-82*, 237.
24. Dong, H.; Ai, X. P.; Yang, H. X. *Electrochem. Commun.* **2003**, *5*, 952.
25. Zhang, J.; Shui, J. L.; Zhang, S. L.; Wei, X.; Xiang, Y. J.; Xie, S.; Zhu, C. F.; Chen, C. H. *Journal of Alloys and Compounds* **2005**, *391*, 212.
26. Jayaprakash, J. N.; Kalaiselvi, N.; Doh, C. H. *Intermetallics* **2007**, *15*, 442.
27. Zhang, Z. N.; Huang, P. X.; Li, G. R.; Yan, T. Y.; Pan, G. L.; Gao, X. P. *Electrochem. Commun.* **2007**, *9*, 713.
28. Rock, N. L.; Kumta, P. N. *J. Power Sources* **2007**, *164*, 829.
29. Wang, K.; He, X.; Mang, L.; Ren, J.; Jiang, C.; Wan, C. *Solid State Ionics* **2007**, *178*, 115.
30. Kalaiselvi, N.; Doh, C. H.; Park, C. W.; Moon, S. I.; Yun, M. S. *Electrochem. Commun.* **2004**, *9*, 1110.